Ribozyme-Catalyzed Dipeptide Synthesis in Monovalent Metal Ions Alone†

Lele Sun,‡ Zhiyong Cui,§ Chunfang Li, Shufang Huang, and Biliang Zhang*

Laboratory of RNA Chemical Biology, Guangzhou Institute of Biomedicine and Health, Chinese Academy of Sciences, Guangzhou Science Park, Guangzhou, China 510663

Received September 26, 2006; Revised Manuscript Received February 1, 2007

ABSTRACT: Previously we have identified a highly active ribozyme (R180, *cis* ribozyme) that can catalyze dipeptide synthesis using *N*-biotinylcaproyl-aminoacyl-adenylate anhydride (Bio-aa-5′-AMP) as its substrate. In this work, we re-engineered the *cis* R180 ribozyme into a 158-nt *trans* ribozyme (TR158) and designed a new substrate (5′-Phe-linker-20-mer). First, the metal ion requirements were examined and compared between the two ribozymes. Both R180 and TR158 ribozymes were active in Mg^{2+} and Ca^{2+} but inert with Zn^{2+}, Cu^{2+}, Mn^{2+}, and Co^{2+}. It is intriguing that both ribozymes were highly active in Li^+, Na^+, or K^+ alone but showed very low activity with NH_4^+. The two ribozymes showed similar linear concentration dependence on Li^+ and K^+, while they displayed different dependency behavior on Mg^{2+}. Moreover, by using the *trans* system, the detailed kinetic studies and pH dependent experiments were performed in either 10 mM Mg^{2+} or 1.0 M Li^+. Analysis of k_{cat} and K_m values obtained at different pHs (6.0 to 9.0) indicated that it is the catalytic activity of the ribozyme but not the substrate binding affinity that changes significantly with pH. The slopes of the linear parts of the pH−rate plots were close to 1.0 in both Mg^{2+}- and Li^+-mediated reactions, suggesting that one proton transfer is involved in the rate-limiting step of catalysis. Overall, our results suggest that Mg^{2+} and Li^+ function similarly in the ribozyme-catalyzed dipeptide synthesis.

Metal ions, particularly divalent metal ions, contribute to ribozyme catalysis by either facilitating structural folding or participating in the chemical step of the reactions (*1*−*4*). It was once believed that all ribozymes are metalloenzymes that require divalent metal ions for activity (*5*). For instance, individual groups have proposed that the *Tetrahymena thermophila* group I intron performs self-splicing through either a three-metal-ion (*6*) or two-metal-ion mechanism (*7*, *8*). Divalent metal ions have also been considered essential for catalysis in hammerhead and HDV[1] ribozymes (*9*−*12*). However, recent studies revealed that some small natural ribozymes including hammerhead, HDV, hairpin, and VS ribozymes can act in the absence of divalent metal ions (*13*−*20*). Both hammerhead and HDV ribozymes are active in high concentrations of monovalent metal ions alone, suggesting that the direct catalytic role of divalent metal ions in these ribozymes could be minor and both kinds of metal ions might promote the reactions by facilitating correct conformation. Subsequent investigations showed similar pH−rate profiles in the reactions with Mg^{2+} and Li^+ in both ribozymes (*14*, *20*). Yet, activities in Li^+ were 100- to 1000-fold lower than those in Mg^{2+} in hammerhead and HDV catalysis. These findings strongly support the idea that monovalent metal ions can partially replace divalent metal ions in some small natural ribozymes, and suggest that a high positive charge density is the fundamental requirement for these ribozymes to perform catalysis.

Artificial ribozymes have been isolated *in vitro* to catalyze various biochemical and chemical reactions, but little is known about the mechanistic aspects of the reactions catalyzed by *in vitro* selected ribozymes. Some studies have been conducted to elucidate the functions of metal ions in the *in vitro* selected ribozymes (*21*−*25*). Two coevolved acyl-transferase ribozymes exhibit variance in metal ion dependence and coordination (*23*), suggesting that the microenvironment in the tertiary structures has an influence on the multiple modes of metal ions. More interestingly, it is found that the aminoacyl-tRNA synthetase ribozyme is active in high concentration of monovalent metal ions alone and the activity in 2.5 M Li^+ or Na^+ is even comparable to that in 0.1 M Mg^{2+} (*24*). Thus, not only the natural ribozymes but also some artificial ribozymes are able to perform catalysis in monovalent metal ions alone.

Most of the naturally occurring ribozymes catalyze reactions at a phosphorus center except the ribosome, which catalyzes peptide bond formation at a carbon center. However, the investigation of the exact mechanism of the ribosomal peptidyl transfer reaction has not been successful

† This research has been supported by the Worcester Foundation and GIBH startup fund.

* To whom correspondence should be addressed: Laboratory of RNA Chemical Biology, Guangzhou Institute of Biomedicine and Health, Chinese Academy of Sciences, Guangzhou Science Park, Guangzhou, China 510663. Phone: +86 (20) 3229-0708. Fax: +86 (20) 3229-0606. E-mail: zhang_biliang@gibh.org.

‡ Current address: Center of Computational and Integrative Biology, Massachusetts General Hospital, Harvard Medical School, Boston, MA.

§ Current address: Department of Medicine, Dartmouth Medical School, Hanover, NH 03755.

[1] Abbreviations: Bio-aa-5′-AMP, *N*-biotinylcaproyl-aminoacyl-adenylate anhydride; dNTPs, deoxyribonucleotide-triphosphates; EDTA, ethylenediaminetetraacetic acid; GMPS, guanosine-5′-monophosphorothioate; HDV, hepatitis delta virus; HEPES, *N*-(2-hydroxyethyl)-piperazine-*N*′-2-ethanesulfonic acid; MES, 2-(*N*-morpholino)ethanesulfonic acid; NTPs, ribonucleotide-triphosphates; PCP, peptidyl carrier proteins; VS, Varkud satellite; TR158, 158-nt *trans* ribozyme; Tris, tris(hydroxymethyl)aminomethane.

10.1021/bi061995m CCC: $37.00
Published on Web 03/02/2007

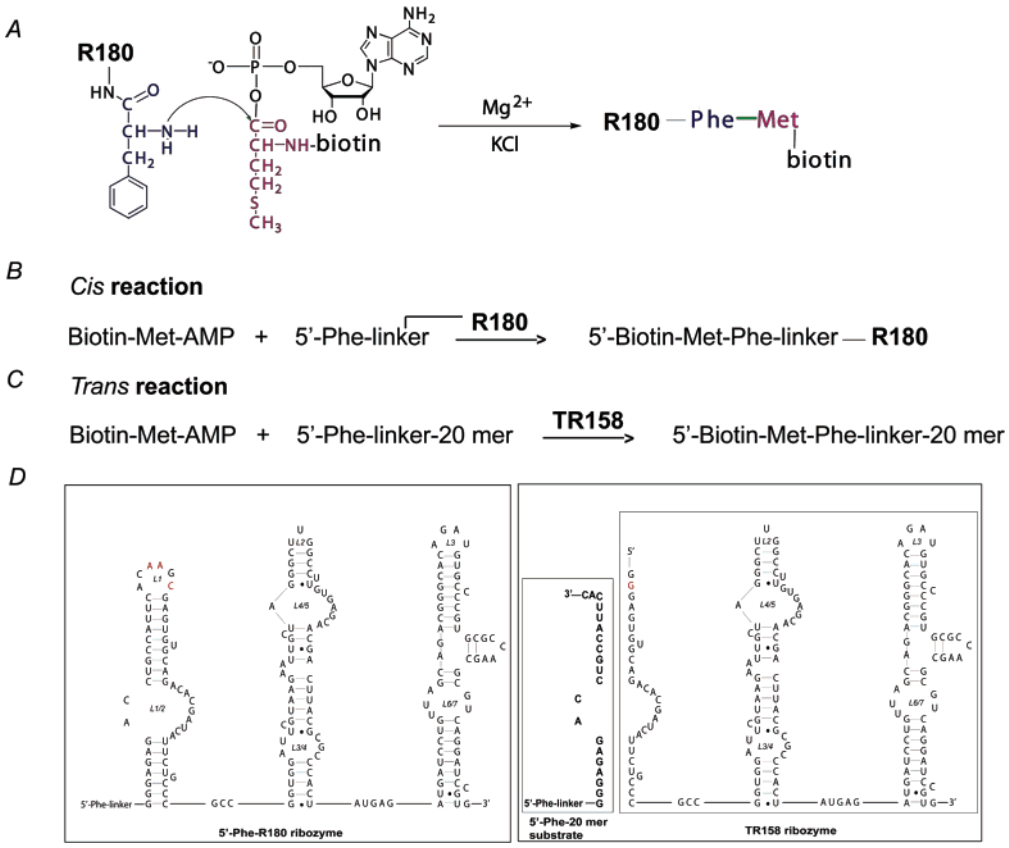

FIGURE 1: (A) Chemical reaction catalyzed by R180 ribozyme. (B) Schematic peptide bond-forming reaction catalyzed by the R180 ribozyme (*cis*-reaction). (C) Schematic peptide bond-forming reaction catalyzed by the TR158 ribozyme (*trans*-reaction). (D) Structure comparison of *cis* and *trans* ribozymes. The R180 ribozyme is prelinked to the Phe substrate. The TR158 ribozyme is 22-nt shorter than the R180 ribozyme at the 5′ end and C24 is mutated to G to create three Gs at the 5′ end of the RNA. The new substrate for the *trans* ribozyme was designed as a 20-mer RNA oligonucleotide (5′-GGGAGAGACCUGCCAUUCAC-3′) linked with phenylalanine at the 5′ end (bold).

due to the complexity of the ribosome system (*26*−*31*). Ribozymes catalyzing reactions at a nonphosphorus center have been isolated *in vitro*, such as the self-alkylating ribozyme (*32*), acyl-transferase ribozyme (*21*, *33*), self-aminoacylating ribozyme (*34*), amide synthetase (*35*), and peptide-synthesizing ribozymes (*36*, *37*). The isolation of peptide-synthesizing ribozymes has provided strong evidence for the hypothesized "RNA world" and shed lights on elucidating the mechanism of ribosomal peptidyl transfer reaction.

The R180 ribozyme catalyzes dipeptide synthesis using *N*-biotinyl-caproyl-aminoacyl-adenylate anhydride (Bio-aa-5′-AMP) as its substrate (*37*, Figure 1A). In the present study, we have re-engineered the R180 system into a trimolecular reaction in which the modified ribozyme (TR158) was physically separated from the two amino acid substrates (Bio-Met-AMP and Phe-linker-20-mer) prior to the catalytic reaction. The R180 and TR158 ribozymes were examined for their metal ion requirements and pH dependence of dipeptide synthesis. Although R180 was selected in the presence of both divalent metal ion (Mg^{2+}) and monovalent metal ion (K^+), both R180 and TR158 were active in monovalent metal ions alone (Li^+, Na^+, or K^+). These two ribozymes displayed similar dependency patterns for monovalent metal ions but showed disagreement for divalent metal ions. Kinetic studies and pH dependence experiments were performed in the TR158-catalyzed reaction to investigate the function of metal ions and the catalytic mechanism of dipeptide formation. Our work also provided more insights into the multiple roles of metal ions in the artificial ribozyme-catalyzed reactions.

RESULTS

Cis- and Trans-Reactions of the Ribozyme-Catalyzed Dipeptide Synthesis. The R180 ribozyme-catalyzed peptide bond formation was a bimolecular reaction with one amino acid (phenylalanine) covalently linked to the 5′ end of the ribozyme as a peptidyl acceptor and the other substrate (Bio-Met-AMP anhydride) as a peptidyl donor (Figure 1B). In order to mimic enzymatic reactions in which the enzyme is physically separated from its substrate prior to the binding and chemical steps, we designed a trimolecular reaction in which neither of the two amino acid substrates was prelinked to the ribozyme. Hence, we call the prototype bimolecular reaction the "*cis*-reaction" and the newly designed trimolecular reaction the "*trans*-reaction".

Design of the *trans*-reaction system was based on the secondary structure model of R180. This *trans* system contains three components: TR158 ribozyme (158 nt), 5′-Phe-linker-20-mer, and Bio-Met-AMP anhydride (Figure 1C). A new substrate (5′-Phe-linker-20-mer) was created as a 20-mer RNA oligonucleotide (5′-GGGAGAGACCUGCCAUUCAC-3′) linked with a phenylalanine at its 5′ end (Figure 1D). Correspondingly, the *trans* ribozyme (TR158) was generated by truncating 22 nucleotides at the 5′ end of R180 and the cytosine at position 24 was mutated to guanine to obtain three consecutive Gs at the 5′ end of the *trans* ribozyme.

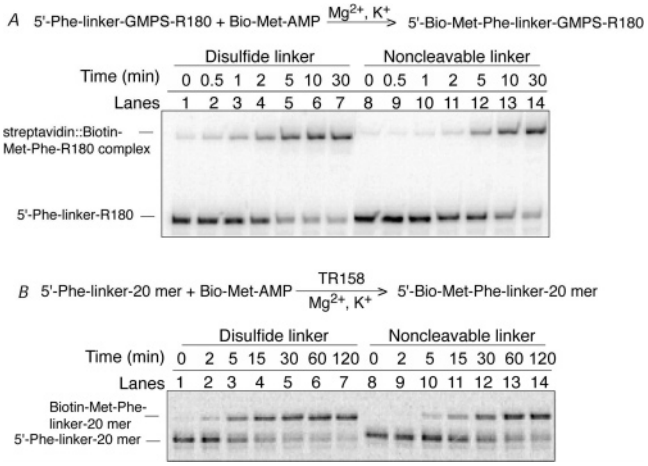

FIGURE 2: Autoradiograms of *cis*- and *trans*-reaction systems catalyzed by R180 and TR158 ribozymes in the presence of 100 mM Mg^{2+}, 300 mM K^+, and 500 μM Biotin-Met-AMP. (A) *Cis*-reaction: The top band corresponds to the product 5′-Bio-Met-Phe-R180 complexed with streptavidin, and the low band corresponds to the inactive R180 ribozymes (5′-Phe-R180). (B) *Trans*-reaction: The top band corresponds to the formed dipeptide linked to the 5′ end of the 20-mer substrates (5′-Bio-Met-Phe-20-mer), and the lower band corresponds to the 5′-Phe-20-mer substrate.

The catalytic activity of peptide bond formation was compared between the *cis* and the *trans* systems. Reactions were carried out with 0.5 μM 5′-Phe-R180 ribozymes for *cis*-reactions or 10 μM TR158 ribozymes and 0.1 μM 5′-Phe-linker-20-mer for *trans*-reactions in the presence of 100 mM Mg^{2+}, 300 mM K^+, and 500 μM Bio-Met-AMP. In the *cis*-reaction system, phenylalanine was linked to the 5′ end of the R180 ribozyme via either a disulfide linker (-$NH(CH_2)_2$-SS-$(CH_2)_2NHC(O)CH_2$-) or a noncleavable linker (-$NH(CH_2)_6NHC(O)CH_2$-), while in the *trans*-reaction system, phenylalanine was linked to the 5′ end of 20-mer oligonucleotide with either the disulfide linker or a noncleavable linker. Figure 2 shows the typical gel-shift assays for analyzing the ribozyme-catalyzed reactions. In the *cis*-reactions (Figure 2A), the top band corresponded to the complex of the biotinylated dipeptide attached to the 5′ end of the R180 RNA (5′-Bio-Met-Phe-R180) with streptavidin, and the low band corresponded to 5′-Phe-linker-R180 RNA. In the *trans*-reactions (Figure 2B), the top band was the formed dipeptide linked to the 5′ end of the 20-mer substrates (5′-Bio-Met-Phe-linker-20-mer), and the low band represented the 5′-Phe-linker-20-mer substrates. The R180 and TR158 ribozymes were both fully active for dipeptide synthesis with over 80% yield at the reaction's final extent. The observed rate constants of dipeptide formation were 0.51 min^{-1} for the *cis*-reaction with a disulfide linker, 0.14 min^{-1} for the *cis*-reaction with a noncleavable linker, 0.21 min^{-1} for the *trans*-reaction with a disulfide linker, and 0.081 min^{-1} for the *trans*-reaction with a noncleavable linker. The ribozyme activities in the *cis*-reactions were higher than those in the *trans*-reactions, and the activities with the disulfide linker were higher than those with the noncleavable linker.

Despite its lower activity, we introduced the *trans* system for several reasons. First, the *trans*-reaction mimics true enzymatic reaction, in which the two substrates are physically separated from the ribozymes. Second, the *trans* system has a unique advantage in kinetic studies. Unlike the *cis* system in which the Bio-Met-AMP substrate always competes with the reaction product (Bio-Met-Phe-R180) in binding with streptavidin, the *trans* system does not require streptavidin for product detection and thus allows more thorough kinetic measurements at high concentrations of substrates. Therefore, in the following experiments, we chose the *trans*-reaction system with the noncleavable linker (more stable than the disulfide linker) for detailed characterization of the ribozyme-catalyzed dipeptide synthesis. Parallel experiments were performed in the *cis*-reaction system with the disulfide linker in order to be consistent with previous publications.

Metal Ion Requirements for R180 and TR158 Ribozymes. The R180 ribozyme was isolated in the presence of both divalent and monovalent metal ions (*37*). To investigate the metal ion specificity of dipeptide synthesis catalyzed by the R180 or TR158 ribozymes, reactions were performed with a single kind of metal ion in each experiment. First, six different divalent metal ions (Mg^{2+}, Ca^{2+}, Zn^{2+}, Cu^{2+}, Mn^{2+}, Co^{2+}) were tested (Figure 3A for R180 and 3C for TR158). In the absence of any metal ion, no product was formed in either system. Both ribozymes were active in Mg^{2+} and Ca^{2+} but not active in the presence of Zn^{2+}, Cu^{2+}, Mn^{2+}, or Co^{2+} alone. To examine whether Mg^{2+} could promote catalysis through the outer-sphere-mediated effect, the reactions were also performed in 10 mM $Co(NH_3)_6^{3+}$ since $Co(NH_3)_6^{3+}$ has a similar atomic geometry to $Mg(H_2O)_6^{2+}$ (*21*, *38*−*39*). However, the ribozymes were not active with $Co(NH_3)_6^{3+}$, suggesting that $Co(NH_3)_6^{3+}$ cannot replace $Mg(H_2O)_6^{2+}$ in catalyzing the dipeptide formation through an outer-sphere-mediated effect (*40*).

We further examined whether the R180 and TR158 ribozymes were active with monovalent cations alone. Four kinds of monovalent ions (Li^+, Na^+, K^+, and NH_4^+) were employed (300 mM each in Figure 3B for R180 and 1.0 M each in Figure 3D for TR158). In these reactions, 25 mM EDTA was included in order to remove any trace amount of divalent metal ions. Interestingly, both ribozymes were highly active in Li^+, Na^+, or K^+ alone; but there was no or very low activity with NH_4^+. These results suggest that R180 does not require divalent metal ions for catalysis and provide more evidence that selected ribozymes can act in monovalent metal ions alone.

The reaction extent and the observed rate constants of peptide bond formation by the R180 or TR158 ribozymes are summarized in Table 1. Generally speaking, the final yields in the *trans* system (80−90%) were higher than those in the *cis* system (50−60%) in the presence of a single metal ion. The *trans*-reaction in Li^+ was more thoroughly completed than in Na^+ and K^+. In the *cis*-reaction, Mg^{2+} and Ca^{2+} showed similar activity but the activity in Li^+ was about 10-fold faster than that in Na^+ and 16-fold faster than that in K^+. In the *trans*-reaction, activity in Ca^{2+} was about 1.5-fold higher than in Mg^{2+} and the observed rate constant in Li^+ was 6−9 times larger than that in Na^+ and K^+. Interestingly, the peptide bond forming reaction in 1.0 M Li^+ was 2-fold faster than that in 10 mM Mg^{2+} or Ca^{2+} in both *cis*- and *trans*-reactions. The order of the ribozyme activity in monovalent ions is $Li^+ > Na^+ > K^+ \gg NH_4^+$. The order of the charge density is $Li^+ > Na^+ > K^+ > NH_4^+$, and the classical ion radius of four monovalent ions is of course $Li^+ < Na^+ < K^+ < NH_4^+$. Li^+ is the most efficient among the tested monovalent metal ions in providing the

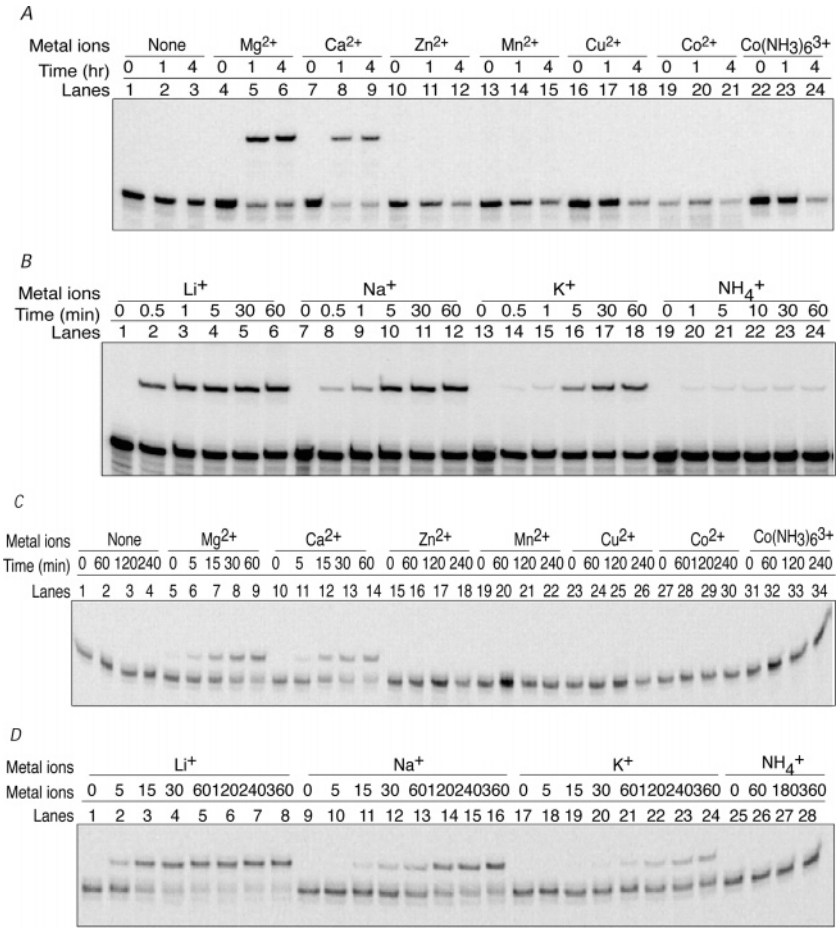

FIGURE 3: Autoradiograms of metal ion specificity of the dipeptide synthesis: (A) *cis* system, 10 mM Mg^{2+}, Ca^{2+}, Zn^{2+}, Cu^{2+}, Mn^{2+}, Co^{2+}, $Co(NH_3)_6^{3+}$; (B) *cis* system, 300 mM Li^+, Na^+, K^+, NH_4^+; (C) *trans* system, 10 mM Mg^{2+}, Ca^{2+}, Zn^{2+}, Cu^{2+}, Mn^{2+}, Co^{2+}, $Co(NH_3)_6^{3+}$; (D) *trans* system, 1.0 M Li^+, Na^+, K^+, NH_4^+.

Table 1: Ribozyme Activity in the Presence of Divalent and Monovalent Metal Ions Measured by *Cis*- and *Trans*-Reaction Systems[a]

		observed rate constants (k_{obs}) ($min^{-}1$)			
no.	metal ions	*cis*-reaction	% yield[b]	*trans*-reaction	% yield[b]
1	10 mM Mg^{2+}	0.12 ± 0.01	62	0.067 ± 0.009	85
2	10 mM Ca^{2+}	0.15 ± 0.03	59	0.099 ± 0.027	88
3	1.0 M Li^+	0.24 ± 0.08	55	0.18 ± 0.03	90
4	1.0 M Na^+	0.026 ± 0.002	50	0.029 ± 0.002	87
5	1.0 M K^+	0.015 ± 0.001	47	0.020 ± 0.001	85

[a] The observed rate constants were measured with both *cis* and *trans* systems in the presence of different metal ions. The dipeptide-forming reactions were carried out with 0.5 μM R180 ribozyme and 100 μM Bio-Met-AMP for the *cis* system and 10 μM TR158 ribozyme, 100 μM Bio-Met-AMP, 0.1 μM 5′-Phe-linker-20-mer for the *trans* system in the presence of 10 mM Mg^{2+} or Ca^{2+}, or 1.0 M Li^+, Na^+, K^+ alone at 25 °C. [b] % yield is the extent of reaction.

positive charge density apparently required by the ribozymes. The ribozymes reached full activity in 1.0 M Li^+, and this concentration was much lower than the reported value (4.0 M) in which the small natural ribozymes still could not reach their full activity as in the presence of divalent metal ions (*13*).

Concentration Dependence of Metal Ions for R180 and TR158 Ribozymes. Ribozyme activities were studied at different concentrations of Mg^{2+}, Li^+, or K^+ in both *cis* and *trans* systems (Figure 4). For the *trans* TR158 reactions, the plot of $\log(k_{obs})$ vs $\log [Mg^{2+}]$ displayed a linear relationship between 1.0 mM and 10 mM Mg^{2+}; then the activity increased slowly at 10−100 mM Mg^{2+} and finally reached a saturation at ≥100 mM Mg^{2+} (Figure 4A). This result is consistent with the described properties of most ribozymes whose activities are saturated at certain concentrations of Mg^{2+} and only a certain amount of Mg^{2+} is required for structural folding and functions of the ribozymes. However, the R180 ribozyme displayed a linear relationship in the k_{obs}−Mg^{2+} plot and no saturation was observed up to 800 mM Mg^{2+} (Figure 4B). The difference of Mg^{2+} concentration dependence between *trans* and *cis* systems might reflect the different microenvironment created by the two systems. Although these two systems gave different Mg^{2+} concentration dependency, the best-fit slopes were 0.60 in the linear part of the *trans*-reaction and 0.41 in the *cis*-reaction, suggesting that both systems are about half-order dependent on the magnesium concentration.

For monovalent metal ions, we observed a linear plot of $\log(k_{obs})$ vs $\log [Li^+]$ or $\log [K^+]$ in both *cis*- and *trans*-reactions (Figure 4). No saturation was observed for the R180 and TR158 ribozyme-catalyzed reactions up to 2000 mM Li^+ and 1875 mM K^+. The slopes of the plots were 2.91 for the Li^+-*cis*-, 2.85 for the Li^+-*trans*-, 3.04 for the K^+-*cis*-, and 2.35 for the K^+-*trans*-reaction. These results indicate that the reactions were about third-order dependent on Li^+ or K^+ concentration. Ribozyme activities at high concentrations of Li^+ or K^+ were comparable to (Figure 4B) or even higher than (Figure 4A) those in Mg^{2+}, suggesting that these

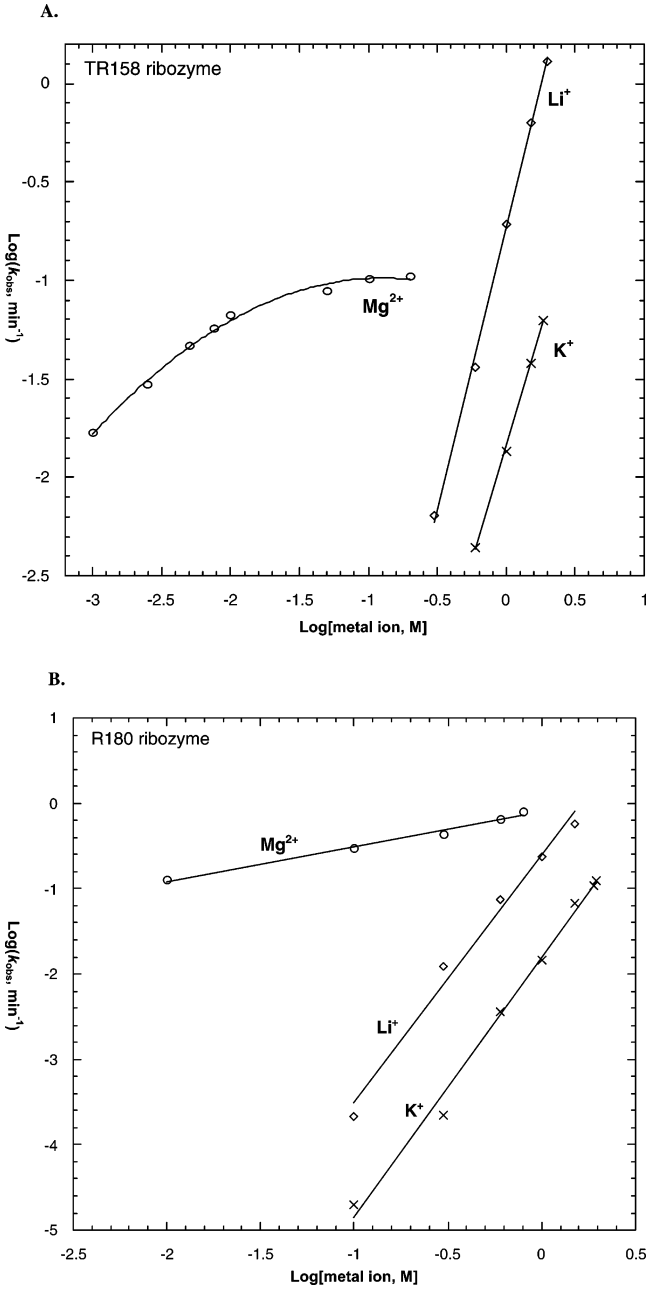

FIGURE 4: Metal ion concentration dependence of the ribozyme catalysis in the presence of Mg^{2+} (○), Li^+ (◇), or K^+ (×) by R180 and TR158 ribozymes. (A) *Trans*-reactions. The lines were drawn as linear with best-fit slopes of 0.6 for Mg^{2+}, 2.85 for Li^+, and 2.35 for K^+. The reaction extents were over 80% for all *trans*-reactions. (B) *Cis*-reactions. The lines were drawn as linear with best-fit slopes of 0.41 for Mg^{2+}, 2.91 for Li^+, and 3.04 for K^+. The reaction extents were 50−60% for *cis*-reactions. All data points were repeated at least twice.

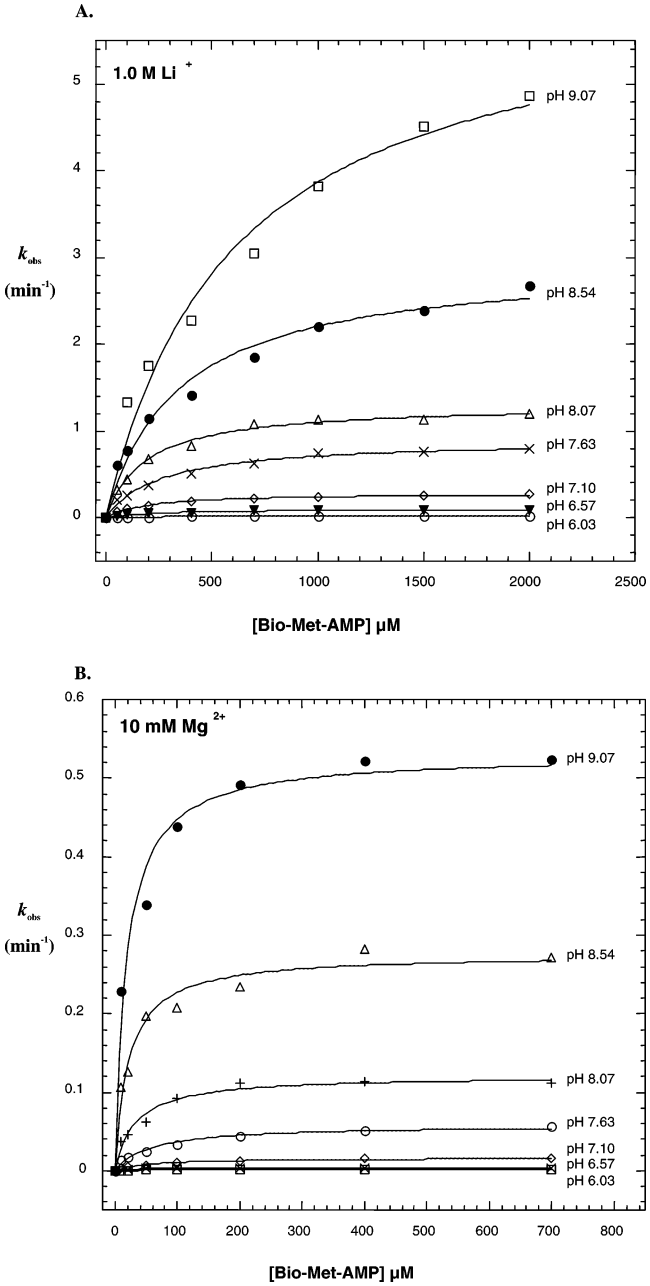

FIGURE 5: Michaelis−Menten curves of the TR158 ribozyme-catalyzed reactions at a various pHs (6.0−9.0) in 1.0 M Li^+ (A) and 10 mM Mg^{2+} (B). The tested Biotin-Met-AMP concentrations range from 50 to 2000 μM. Each data point was repeated al least twice. For both Li^+- and Mg^{2+}-mediated reactions, the final extent of reaction was over 85% at all substrate concentrations. k_{cat} and K_m values were obtained by the best fit of the data to Michaelis−Menten equation of k_{obs} = [substrate] × k_{cat}/([substrate] + K_m) at the different pHs.

monovalent metal ions could fully substitute divalent metal ions in the ribozyme-catalyzed dipeptide synthesis.

pH Dependence of TR158-Catalyzed Dipeptide Formation. We performed kinetic studies at different pHs (6.0−9.0) in either Mg^{2+} or Li^+ by using the *trans* system (Figure 5). k_{cat} and K_m values are summarized in Table 2. In 10 mM Mg^{2+}, K_m reached a maximum of 89 μM at pH 6.0 and a minimum of 17 μM at pH 9.0 and the difference was 5-fold. However, the k_{cat} value was about 200-fold different between the maximum k_{cat} at pH 9.0 (5.2×10^{-1} min^{-1}) and the minimum k_{cat} at pH 6.0 (2.6×10^{-3} min^{-1}). Similar results were also observed in 1.0 M Li^+. K_m reached a maximum of 599 μM at pH 9.0 and a minimum of 197 μM at pH 7.1 with a 3-fold difference, while k_{cat} increased about 200-fold from 3.1×10^{-2} min^{-1} at pH 6.0 to 6.2 min^{-1} at pH 9.0. These results suggest that in either Mg^{2+}- or Li^+-mediated reactions, pH change does not have a great influence on the substrate binding affinity but rather significantly affects the catalytic activity of the ribozyme. Over the entire tested pH range, K_m measured in 1.0 M Li^+ was uniformly higher than that in 10 mM Mg^{2+}, suggesting that the Bio-Met-AMP substrate is less tightly bound to the ribozyme in 1.0 M Li^+ than in 10 mM Mg^{2+}.

Table 2: Kinetic Parameters (k_{cat} and K_m) of the Peptide Bond Formation Catalyzed by the TR158 Ribozyme at Various pHs in the Presence of 10 mM Mg^{2+} or 1.0 M Li^+ [a]

		reaction in 10 mM Mg^{2+}			reaction in 1.0 M Li^+		
no.	pH	k_{cat} (min^{-1})	K_m (μM)	k_{cat}/K_m ($M^{-1}\cdot min^{-1}$)	k_{cat} (min^{-1})	K_m (μM)	k_{cat}/K_m ($M^{-1}\cdot min^{-1}$)
1	6.0	2.6×10^{-3}	89	2.9×10^{1}	3.1×10^{-2}	379	8.3×10^{1}
2	6.6	4.6×10^{-3}	34	1.3×10^{2}	1.1×10^{-1}	289	3.7×10^{2}
3	7.1	1.7×10^{-2}	53	3.1×10^{2}	2.9×10^{-1}	197	1.5×10^{3}
4	7.6	5.8×10^{-2}	58	1.0×10^{3}	9.0×10^{-1}	260	3.4×10^{3}
5	8.1	1.2×10^{-1}	32	3.7×10^{3}	1.4	292	4.7×10^{3}
6	8.5	2.8×10^{-1}	21	1.3×10^{4}	3.0	344	8.6×10^{3}
7	9.1	5.2×10^{-1}	17	3.0×10^{4}	6.2	599	1.0×10^{4}

[a] Kinetic studies were performed under different reaction conditions by *trans*-reaction system. Reactions were carried out with 10 μM TR158 ribozyme, 0.1 μM 5′-Phe-linker-20-mer substrate, and 50 mM pH buffer (MES for pH 6.0−6.5 and for pH 6.5−9.0) in the presence of either 10 mM Mg^{2+} or 1.0 M Li^+. At each specific pH value, the reactions were carried out at different concentrations of the Bio-Met-AMP substrate (50−2000 μM) to obtain k_{cat} and K_m values from Figure 5. The extents of all reactions were over 80%.

pH effect was further investigated by plotting log(k_{cat}) vs pH (Figure 6A). Similar curves were observed in both Mg^{2+}- and Li^+-mediated reactions regardless of the activity difference. Both pH profiles consisted of a linear region at low pH (6.0−8.0) and slightly bent down at higher pH (8.0−9.0). Log(k_{obs}) vs pH (Figure 6B) also exhibited a similar pH-dependence relationship as in the log(k_{cat}) vs pH profiles. The slopes of the linear parts of all pH profiles were close to 1, suggesting that one proton transfer might be involved in the rate-limiting step of the ribozyme-catalyzed dipeptide formation. At high pH, the profiles seemed to bend down a little bit but a plateau was not observed. It is difficult to explore whether the curve will reach a plateau because of the nonspecific degradation of the ribozymes at high pH (>9.0). To exclude the possibility that the slowdown of the reaction is due to the hydrolysis of the Bio-Met-AMP substrate, we examined the substrate stability at different pHs by capillary electrophoresis (unpublished data). Under all tested pH conditions (6.0−9.0), the half-life of Bio-Met-AMP was longer than the time required for the reaction to reach over 80% completion. Considering that Bio-Met-AMP at the minimum concentration of 10 μM is still in large excess (≥100-fold) over 5′-Phe-linker-20-mer (0.1 μM), the hydrolysis of Bio-Met-AMP would not contribute significantly to the chemical rates at high pH. Therefore, we still cannot exclude the possibility that the bending down of the curve reflects the pH-insensitive region of the reaction.

Solvent Isotope Effect of TR158-Catalyzed Reactions. To further examine whether proton transfer is involved in the rate-limiting step of dipeptide formation, we measured isotope effect of D_2O for the *trans* TR158 ribozyme in the pH range 6.0−9.0. Isotope effects have proven to be powerful and sensitive probes for dissecting the mechanistic chemistry and the transition state structures of ribozyme-catalyzed reactions (*41*−*43*). pD dependence experiments were performed the same as pH-dependence experiments except that all active hydrogen atoms were replaced by deuterium. Similarly to the pH profiles, all pD profiles exhibited a linear part at pH 6.0 to 8.5 and a slight curvature at pH 8.5−9.0 in both Mg^{2+}- and Li^+-mediated reactions (Figure 7). The activities in D_2O were uniformly lower than those in H_2O by about 10-fold. In the ribozyme-catalyzed reactions, an isotope effect of more than 7-fold usually implicates that proton transfer is involved in catalysis (*41*). Therefore, our experiments suggest that proton transfer might be involved in the rate-limiting step during peptide bond formation catalyzed by the TR158 ribozyme.

DISCUSSION

Laboratory-evolved ribozymes usually require divalent metal ions for activity since they are isolated in the presence of divalent metal ions under strictly defined conditions, which also include other factors such as monovalent metal ions and spermidine. The R180 ribozyme was isolated in the presence of Mg^{2+} and K^+ (*37*, Figure 1A). However, R180, as well as its re-engineered form TR158, were both active in the presence of monovalent metal ions (Li^+, Na^+, or K^+) alone (Figure 3). The activities achieved at 1.0 M Li^+ were equal to (in R180) or even higher than (in TR158) those at 10 mM Mg^{2+} (Table 1), suggesting that R180 and TR158 ribozymes are highly active in monovalent metal ions alone, and do not require divalent metal ions to obtain full activity. In comparison, some small naturally occurring ribozymes are not very active even at 4.0 M Li^+ and the presence of Mg^{2+} is required for these ribozymes to gain full activity (*44*). The activity of aminoacyl-tRNA synthetase ribozyme in 2.5 M Li^+ or Na^+ is comparable to that in 0.1 M Mg^{2+} (*24*). Our results support the idea that not all ribozymes require divalent metal ions for activity and the positive charge supplied by the metal cations is the fundamental requirement for certain ribozymes to perform catalysis.

To compare the roles of divalent and monovalent metal ions in the ribozyme-catalyzed reactions, we have determined concentration dependence of different metal ions (Mg^{2+}, Li^+, or K^+) and pH dependence in either Mg^{2+} or Li^+ alone. Our data suggest that divalent Mg^{2+} and monovalent Li^+ might function similarly based on the following evidence. First, ribozyme activity displayed a linear relationship with either Mg^{2+} or Li^+ (Figure 4), suggesting that the ribozyme requirements for divalent and monovalent metal ions are similar. The requirement of both ribozymes for much higher concentrations of Li^+ than Mg^{2+} may arise because the charge density of Mg^{2+} is much higher than that of Li^+ (*45*). Mg^{2+} exhibited different dependency behavior from Li^+ (half-order dependent on Mg^{2+} while third-order on Li^+), which may reflect the different ability of divalent and monovalent metal ions to interact and neutralize the charge in the polyanionic ribozyme•substrate complex. A similar phenomenon is also observed in the hammerhead ribozyme (first-order dependent on Mg^{2+} and second-order dependent

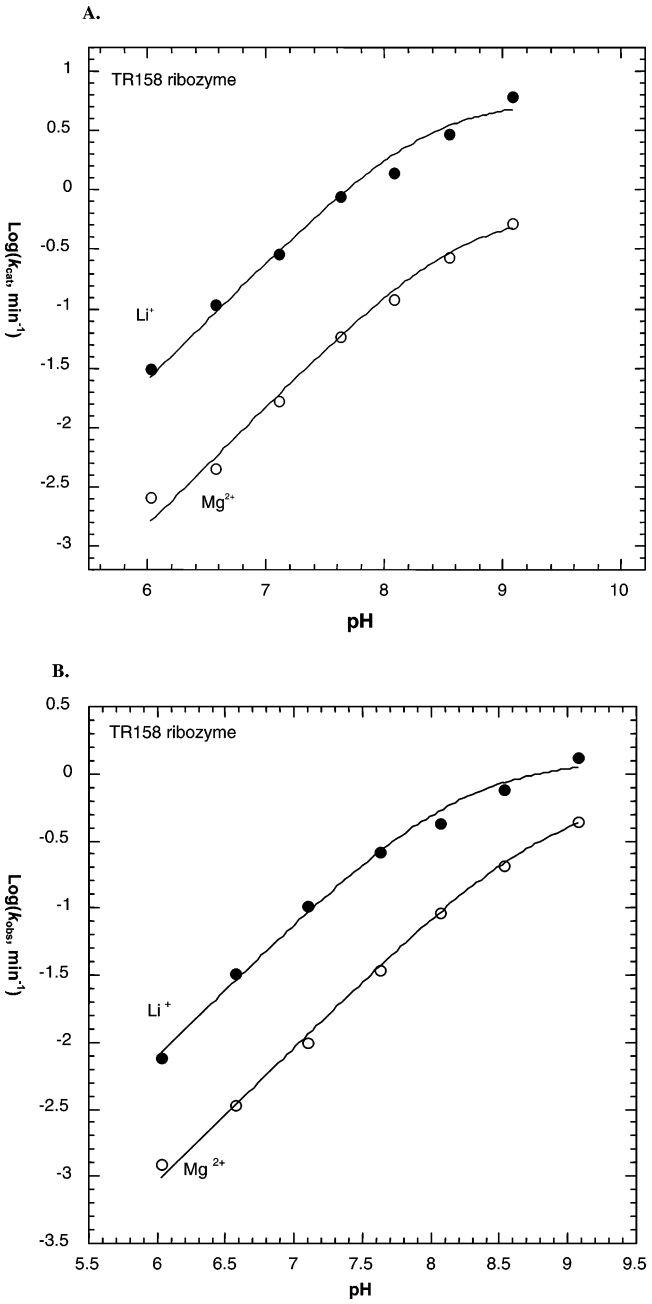

FIGURE 6: pH dependence of TR158-catalyzed peptide bond formation in 10 mM Mg^{2+} (○) or 1.0 M Li^+ (●). The pH buffers are 50 mM MES buffer from pH 5.5 to 6.0 and 50 mM Bis·Tris propane from pH 6.5 to 9.0. (A) Log(k_{cat}) vs pH profiles. The slopes of the linear parts were 1.0 for Mg^{2+} and 1.0 for Li^+. (B) Log(k_{obs}) vs pH profiles. The observed rate constants were obtained at 500 μM Bio-Met-AMP. The slopes of the linear parts were 0.87 for Mg^{2+} and 0.90 for Li^+.

on Li^+) (*15*). Second, the shapes of pH dependence profiles in either Mg^{2+} or Li^+ were almost identical except the activity difference (Figure 6), implying a similar requirement for these two metal ions by the catalytic step of ribozyme catalysis. The lack of activity in $Co(NH_3)_6^{3+}$ rules out the possibility that Mg^{2+} binds through an outer-sphere coordination site to promote catalysis. Both divalent and monovalent metal ions can coordinate to the H_2O group, but they differ in that divalent metal ions can lower the pK_a of the H_2O group while monovalent metal ions cannot.

The catalytic mechanism of peptide bond formation catalyzed by the ribozymes has been investigated by using

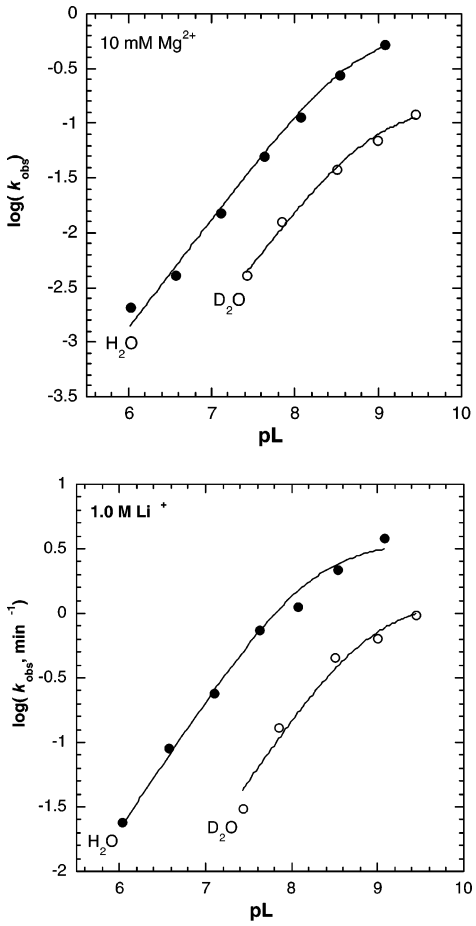

FIGURE 7: Solvent isotope effects of peptide bond formation catalyzed by TR158 ribozyme in 10 mM Mg^{2+} (A) and 1.0 M Li^+ (B). Reactions were performed in either H_2O (●) or D_2O (○).

the *trans* system. The *trans* system allows more thorough kinetic studies and some experimental designs that are not possible with the *cis* system. pH dependence and solvent isotope effect suggest that one proton transfer is involved in the rate-limiting step of TR158-catalyzed peptide bond formation (Figure 6 and Figure 7). It is likely that the amino group on phenylalanine acts as a nucleophile to attack the carbonyl carbon on methionine and form a tetrahedral intermediate. Deprotonation of the NH_2 group then probably leads to the cleavage of the C−O bond to give the dipeptide product.

Successful isolation of artificial ribozymes that can catalyze various kinds of chemical and biochemical reactions has strongly supported the "RNA world" hypothesis. However, such laboratory-evolved ribozymes need not be chemically similar or even directly relevant to the actual molecular assemblies that led to the origin of life on earth (*46*). Therefore, we need to take great caution in using the R180 system as a model to interpret the ribosomal peptidyl transfer reaction. The chemical forms of the substrates are different between the R180 and the ribosome systems. In the R180 system, the substrate is an analogue of aminoacyl-adenylate in which the amino acid is linked to the 5′ phosphate of adenosine, while in the ribosome, amino acid is charged to the 3′ position of the terminal adenosine in tRNA through an ester bond. That is to say, the R180 ribozyme catalyzes uncoded dipeptide synthesis while the ribosome catalyzes coded protein synthesis. Thus, it is likely that these two

systems catalyze peptide bond formation via different mechanisms. From an evolutionary point of view, uncoded protein synthesis might have preceded the emergence of coded protein synthesis. Because aminoacyl-adenylate is a universal intermediate before amino acid is charged to either tRNA or PCP, it may have played a role in uncoded protein synthesis in an ancient world. Therefore, the R180 system may provide a good system to investigate the peptidyl transfer reaction in uncoded protein synthesis.

MATERIALS AND METHODS

General Materials. Inorganic salts and chemical reagents were purchased from Sigma, Aldrich, or Acros. HEPES (*N*-(2-hydroxyethyl)-piperazine-*N*′-2-ethanesulfonic acid), MES (2-(*N*-morpholino)ethanesulfonic acid), Tris (tris(hydroxymethyl)aminomethane), Bis-Tris propane, and EDTA (ethylenediaminetetraacetic acid) were purchased from Sigma. Guanosine-5′-monophosphorothioate (GMPS) was purchased from Biotech GmbH, Germany. Deoxyribonucleotide-triphosphates (dNTPs) and ribonucleotide-triphosphates (NTPs) were purchased from Amersham, Streptavidin was from Pierce, Taq DNA polymerase was from New England Biolabs, and α-^{32}P-ATP and γ-^{35}S-ATP were from New Life Science Products. The primers used for producing cDNA templates were purchased from Operon. The instrument used for Capillary Electrophoresis was the P/ACE System MDQ from Beckman. Autoradiogram analysis was performed on a Molecular Dynamic PhosphorImager.

Ribozyme Preparation. The R180 and TR158 ribozymes were prepared by runoff transcription using the corresponding cDNA templates. The R180 ribozyme was re-engineered by deleting 22 nucleotides at the 5′ end and mutating C24 to G. The resulted *trans* ribozyme (TR158) was 22-nt shorter than the R180 ribozyme. Transcription reactions were carried out in 40 mM Tris·HCl (pH 7.4), 12 mM $MgCl_2$, 40 mM DTT, 4 mM spermidine, and 0.08% Triton X-100 with 5 μg of DNA template per 100 μL reaction at 37 °C. The ^{32}P-labeled R180 ribozymes were synthesized in the presence of 10 μCi/200 μL reaction of α-^{32}P-ATP, 2 mM each ATP/GTP/CTP/UTP, and 32 mM guanosine-5′-monophosphorothioate (GMPS). The TR158 ribozymes were synthesized in the presence of 2 mM each ATP/GTP/CTP/UTP only. Both ^{32}P-labeled R180 ribozymes and nonlabeled TR158 ribozymes were purified by 8% polyacrylamide/7.5 M urea denaturing gel electrophoresis (PAGE). Ribozymes were visualized by UV. The gel containing the ribozymes was excised, squeezed through a syringe, and soaked in TE buffer (10 mM Tris and 1 mM EDTA buffer, pH 7.4) at 4 °C overnight. Then the soaking solution was separated from the gel by filtration and centrifugation at 5000*g* for 10 min. Both ribozymes were precipitated by 250 mM NaCl and cold ethanol in dry ice for 2 h. The TR158 ribozymes were then resuspended in deionized water and stored at −20 °C. The ^{32}P-labeled 5′-GMPS-R180 RNAs were further reacted with 100 mM either Phe-NH$(CH_2)_2$-S-S-$(CH_2)_2$NH-C(O)CH_2Br (disulfide linker) (*22*) or Phe-NH$(CH_2)_6$NH-C(O)CH_2Br (noncleavable linker) (*37*) in the presence of 40 mM HEPES (pH 7.8), 150 mM NaCl, and 10 mM EDTA. Both linkers were chemically synthesized in the lab. The coupling reactions were carried out by continuously rotating at room temperature for 3 h. Then, the reaction mixtures were extracted by phenol/chloroform to remove excess linker. Finally, the 5′-Phe-R180 ribozymes were precipitated in cold ethanol, resuspended in deionized water, and stored at −20 °C for kinetic studies.

Preparation of 5′-Phe-linker-20-mer Substrates for the Trans-Reaction. The 20-mer RNA oligonucleotide (GGGAGAGACCUGCCAUUCAC, the first 20-nt sequence at the 5′ end of the R180 ribozyme) was chemically synthesized and labeled with γ-^{35}S-ATP by T4 polynucleotide kinase (PNK). The labeling reaction was performed with 10 nmol of 20-mer RNA oligonucleotides, 200 units of PNK, and 200 pmol (250 μCi) of γ-^{35}S-ATP in the presence of 70 mM Tris-HCl (pH 7.6), 10 mM $MgCl_2$, and 5 mM DTT at 37 °C for 2 h. Then an excess of γ-thiophosphate-ATP (4.5 mM) was added in order to convert all 20-mer RNA oligonucleotides into 5′-thiophospate-20-mer RNAs. The ^{35}S-labeled 20-mer RNA oligonucleotides were purified by 20% polyacrylamide/7.5 M urea denaturing gel and linked to either disulfide linker or noncleavable linker as described above. The resulting 5′-Phe-linker-20-mer substrates were stored at −20 °C for the *trans*-reactions.

Kinetics Studies. For *cis*-reactions, 0.5 μM R180 ribozyme was preincubated with 1−1000 mM metal cations in the presence of 50 mM Bis·Tris propane buffer (pH 7.5) at 50 °C for 10 min, and then the mixture was slowly cooled down to room temperature. The reaction was initiated by addition of Bio-Met-AMP anhydride substrate at 25 °C. A 1 μL aliquot of the reaction mixture was removed from the reaction tube at the specific time points, quenched with 2 μL of quench buffer (50 mM HEPES, pH 7.5, 25 mM EDTA, 90% formamide dye with 0.09% bromphenol blue and 0.09% xylene cyanol FF), and stored in dry ice. Each sample was incubated with 10 μg of streptavidin at room temperature for 15−20 min prior to being loaded on 8% polyacrylamide/7.5 M urea denaturing gel. Reaction products were quantitated by Molecular Dynamics Phosphorimager, and the fraction of the product relative to the total reactant was plotted against different time points. The observed rate constants (k_{obs}) were obtained by curve fitting in KaleidaGraph.

For *trans*-reactions, 10 μM TR158 ribozyme was mixed with 0.1 μM 5′-Phe-linker-20 mer substrate in the presence of 1−1000 mM metal cations and 50 mM Bis•Tris propane buffer (pH 7.5). Other conditions were the same as described above except that all samples were directly loaded onto 20% polyacrylamide/7.5 M urea denaturing gel without streptavidin incubation.

Metal Cation Dependence Experiments. Kinetic analyses were performed with different species and various concentrations of metal cations. The metal cation requirement for the ribozyme-catalyzed reaction was examined by both *cis*- and *trans*-reaction systems. Reactions were performed with 0.5 μM 5′-Phe-R180 ribozyme for *cis*-reactions or 10 μM TR158 ribozyme and 0.1 μM 5′-Phe-linker-20-mer for *trans*-reaction, and 500 μM Bio-Met-AMP substrate in the presence of 50 mM Bis·Tris propane buffer (pH 7.4) and 10 mM Mg^{2+}, Ca^{2+}, Zn^{2+}, Cu^{2+}, Mn^{2+}, Co^{2+}, $Co(NH_3)_6^{3+}$, or 1.0 M Li^+, Na^+, K^+, NH_4^+. The metal cation concentration dependence was assayed in the presence of 1−800 mM Mg^{2+}, 300−2000 mM Li^+, or 600−1875 mM K^+. For monovalent cations, 25 mM EDTA was included in the reactions. The observed rate constants (k_{obs}) were obtained

for each specific concentration with a single kind of metal ion. The data were analyzed by KaleidaGraph software.

pH Dependence and Isotope Exchange Experiments. Kinetic analyses were performed as described above at different pHs with both *cis*- and *trans*-reaction systems. The pH buffers used in the reactions were 50 mM MES for pH 5.5−6.5 and 50 mM Bis·Tris propane for pH 6.5−9.0. For *cis*-reactions, pH dependence assays were performed with 0.5 μM R180 ribozyme, 100 μM Bio-Met-AMP, and 50 mM buffer in the presence of either 100 mM Mg^{2+} or 1.0 M Li^{+}. The observed rate constants were log plotted against pH [log(k_{obs}) vs pH]. For *trans*-reactions, pH dependence was examined with 10 μM TR158 ribozyme, 0.1 μM 5′-Phe-20-mer substrate, 100 μM Bio-Met-AMP, and 50 mM pH buffer in the presence of either 10 mM Mg^{2+} or 1.0 M Li^{+}. At each specific pH value, the reactions were carried out at different concentrations of Bio-Met-AMP substrate (10−700 μM for Mg^{2+}, 50−2000 for Li^{+}) to generate Michaelis−Menten curves. k_{cat} and K_m values were obtained from the Michaelis−Menten plots at each pH. The relationship between k_{cat} and pH was displayed by plotting log(k_{cat}) vs pH.

For our solvent isotope experiments, all buffers were made in 99.9% D_2O, lyophilized, and redissolved in 99.9% D_2O (repeat twice) to exhaust any exchangeable proton. pD was calculated by adding 0.4 to a pH meter reading (titrated with KOD). Salts, ribozyme, and substrate were lyophilized, dissolved in 99.9% D_2O, and this process was repeated twice. pD dependence experiments were performed as described above.

REFERENCES

1. Feig, A.L., and Uhlenbeck, O.C. (1999). The role of metal ions in RNA biochemistry, in *The RNA world* (Atkins, J. F., Ed.) 2nd ed., pp 287−319, Cold Spring Harbor Laboratory Press, Cold Spring Harbor, NY.
2. Fedor, M. J. (2002) The role of metal ions in RNA catalysis, *Curr. Opin. Struct. Biol. 12*, 289−295.
3. Hanna, R., and Doudna, J. A. (2000) Metal ions in ribozyme folding and catalysis, *Curr. Opin. Chem. Biol. 4*, 166−170.
4. Takagi, Y., Warashina, M., Stec, W. J., Yoshinari, K., and Taira, K. (2001) Recent advances in the elucidation of the mechanism of action of ribozymes, *Nucleic Acids Res. 29* (9), 1815−1834.
5. Pyle, A. M. (1993) Ribozymes: A distinct class of metalloenzymes, *Science 261*, 709−714.
6. Shan, S., Yoshida, A., Sun, S., Piccirilli, J. A., and Herschlag, D. (1999) Three metal ions at the active site of the Tetrahymena group I ribozyme, *Proc. Natl. Acad. Sci. U.S.A. 96*, 12299−12304.
7. Stahley, M. R., and Strobel, S. A. (2005) Structural evidence for a two-metal ion mechanism of group I intron splicing, *Science 309*, 1587−1590.
8. Stahley, M. R., and Strobel, S. A. (2006) RNA splicing: group I intron crystal structures reveal the basis of splice site selection and metal ion catalysis, *Curr. Opin. Struct. Biol. 16*, 319−326.
9. Dahm, A. C., and Uhlenbeck, O. C. (1991) Role of divalent metal ions in the hammerhead RNA cleavage reaction, *Biochemistry 30*, 9464−9469.
10. Dahm, A. C., Derrick, W. B., and Uhlenbeck, O. C. (1993) Evidence for the role of solvated metal hydroxide in the hammerhead cleavage mechanism, *Biochemistry 32*, 13040−13045.
11. Scott, W. G., Murray, J. B., Arnold, J. R. P., Stoddard, B. L., and Klgu, A. (1996) Capturing the structure of a catalytic RNA intermediate: the hammerhead ribozyme, *Science 274*, 2065−2069.
12. Nakano, S., Chadalavada, D. M., and Bevilacqua, P. C. (2000) General acid-base catalysis in the mechanism of a hepatitis delta virus ribozyme, *Science 287*, 1493−1497.
13. Murray, J. B., Seyhan, A. A., Walter, A. G., Burke, J. M., and Scott, W. G. (1998) The hammerhead, hairpin and VS ribozyme-sare catalytically proficient in monovalent cations alone, *Chem. Biol. 5* (10), 587−595.
14. Curtis, E. A., and Bartel, D. P. (2001) The hammerhead cleavage reaction in monovalent cations, *RNA 7*, 546−552.
15. O'Rear, J. L., Wang, S., Feig, A. L., Beigelman, L., Uhlenbeck, O. C., and Herschlag, D. (2001) Comparison of the hammerhead cleavage reactions stimulated by monovalent and divalent cations, *RNA 7*, 537−545.
16. Zhou, J., Zhou, D., Takagi, Y., Kasai, Y., Inoue, A., Baba, T., and Taira, K. (2002) Existence of efficient divalent metal ion-catalyzed and inefficient divalent metal ion-independent channels in reactions catalyzed by a hammerhead ribozyme, *Nucleic Acids Res. 30* (11), 2374−2382.
17. Takagi, Y., and Taira, K. (2002). Analyses of kinetic solvent isotope effects of a hammerhead ribozyme reaction in NH_4^{+} and Li^{+} ions, *Nucleic Acids Res. Suppl.* No. 2, 273−4.
18. Nakano, S., Procter, D. J., and Bevilacqua, P. C. (2001) Mechanistic characterization of the HDV genomic ribozyme: assessing the catalytic and structural contributions of divalent metal ions within a multichannel reaction mechanism, *Biochemistry 40*, 12022−12038.
19. Wadkins, T. S., Shih, I., Perrotta, A. T., and Been, M. D. (2001) A pH-sensitive RNA tertiary interaction affects self-cleavage activity of the HDV ribozymes in the absence of added divalent metal ion, *J. Mol. Biol. 305*, 1045−1055.
20. Perrotta, A. T., and Been, M. D. (2006) HDV ribozyme activity in monovalent cations, *Biochemistry 45*, 11357−11365.
21. Suga, H., Cowan, J. A., and Szostak, J. W. (1998) Unusual metal ion catalysis in an acyl-transferase ribozyme, *Biochemistry 37*, 10118−10125.
22. Zhang, B., and Cech, T. R. (1998) Peptidyl-transferase ribozymes: trans reactions, structural characterization and ribosomal RNA-like features, *Chem. Biol. 5*, 539−553.
23. Vaidya, A., and Suga, H. (2001) Diverse roles of metal ions in acyl-transferase ribozymes, *Biochemistry 40*, 7200−7210.
24. Saito, H., and Suga, H. (2002) Outsphere and innersphere coordinated metal ions in an aminoacyl-tRNA synthetase ribozyme, *Nucleic Acids Res. 30* (23), 5151−5159.
25. Flynn-Charlebois, A., Lee, N., and Suga, H. (2001) A single metal ion plays structural and chemical roles in an aminoacyl-transferase ribozyme, *Biochemistry 40*, 13623−13632.
26. Nissen, P., Hansen, J., Ban, N., Moore, P. B., and Steitz, T. A. (2000) The structural basis of ribosome activity in peptide bond synthesis, *Science 289*, 920−930.
27. Polacek, N., Gaynor, M., Yassin, A., and Mankin, A. S. (2001) Ribosomal peptidyl transferase can withstand mutations at the putative catalytic nucleotide, *Nature 411*, 498−501.
28. Thompson, J., Kim, D. F., O'Connor, M., Lieberman, K. R., Bayfield, M. A., Gregory, S. T., Green, R., Noller, H. F., and Dahlberg, A. E. (1998) Analysis of mutations at residues A2451 and G2447 of 23S rRNA in the peptidyltransferase active site of the 50S ribosomal subunit, *Proc. Natl. Acad. Sci. U.S.A. 98*, 9002−9007.
29. Bayfield, M. A., Dahlberg, A. E., Schulmeister, U., Dorner, S., and Barta, A. (1998) A conformational change in the ribosomal peptidyl transferase center upon active/inactive transition, *Proc. Natl. Acad. Sci. U.S.A. 98*, 10096−10101.
30. Xiong, L., Polacek, N., Sander, P., Bottger, E. C., and Mankin, A. E. (2001) pK_a of adenine 2451 in the ribosomal peptidyl transferase center remains elusive, *RNA 7*, 1365−1369.
31. Muth, G. W., Chen, L., Kosek, A. B., and Strobel, S. A (2001) pH-dependent conformational flexibility within the ribosomal peptidyl transferase center, *RNA 7*, 1403−1415.
32. Wilson, C., and Szostak, J. W. (1995) In vitro evolution of a self-alkylating ribozyme, *Nature 374*, 777−782.
33. Lohse, P. A., and Szostak, J. W. (1996) Ribozyme-catalyzed amino-acid transfer reactions, *Nature 381*, 442−444.
34. Illangasekare, M., and Yarus, M. (1999) A tiny RNA that catalyzes both aminoacyl-RNA and peptidyl-RNA synthesis, *RNA 5* (11), 1482−1489.
35. Wiegand, T. W., Janssen, R. C., and Eaton, B. E. (1997) Selection of RNA amide synthetases, *Chem. Biol. 4* (9), 675−683.
36. Zhang, B., and Cech, T. R. (1997) Peptide bond formation by in vitro selected ribozymes, *Nature 390*, 96−100.
37. Sun, L., Cui, Z., Gottlieb, R. L., and Zhang, B. (2002) A selected ribozyme catalyzing diverse dipeptide synthesis, *Chem. Biol. 9* (5), 619−628.

38. Cate, J. H., and Doudna, J. A. (1996) Metal-binding sites in the major groove of a large ribozyme domain, *Structure 4*, 1221−1229.
39. Kieft, J. S., and Tinoco, J. I. (1997) Solution structure of a metal-binding site in the major groove of RNA complexed with cobalt-(III) hexamine, *Structure 5*, 713−721.
40. Misra, V. K., and Draper, D. E. (1998) On the role of magnesium ions in RNA stability, *Biopolymers 48*, 113−135.
41. Sawata, S., Komiyama, M., and Taira, K. (1995) Kinetic evidence based on solvent isotope effects for the nonexistence of a proton-transfer process in reactions catalyzed by a hammerhead ribozyme: Implication to the double-metal-ion mechanism of catalysis, *J. Am. Chem. Soc. 117*, 2357−2358.
42. Nakano, S., and Bevilacqua, P. C. (2001) Proton inventory of the genomic HDV ribozymes in Mg^{2+}-containing solutions, *J. Am. Chem. Soc. 123*, 11333−11334.
43. Takagi, Y., and Taira, K. (2002) Detection of a proton-transfer process by kinetic solvent isotope effects in NH_4^+-mediated reactions catalyzed by a hammerhead ribozyme, *J. Am. Chem. Soc. 124*, 3850−3852.
44. Murray, J. B., Dunham, C. M., and Scott, W. G. (2002) A pH-dependent conformational change, rather than the chemical step, appears to be rate-limiting in the hammerhead ribozyme cleavage reaction, *J. Mol. Biol. 315*, 121−130.
45. Bhattacharya, P. K. (2005). Thermodynamic and Kinetic Properties of Metal Complexes, in *Metal Ions in Biochemistry*, p 19, Alpha Science Int'l Ltd.
46. Szostak, J. W., Bartel, D. P., and Luisi, P. L. (2001) Synthesizing life, *Nature 409* (6818), 387−390.

BI061995M